CFD Letters www.cfdl.issres.net Vol. 3 (2) – June 2011

A High Order Spectral Volume Method for Equations Containing Third Spatial Derivatives Using an Interior Penalty Formulation

R. Raghavendra[c]
Department of Computer Science, University of Alabama at Huntsville
U.S.A

Received: 05/04/2011 – Revised 02/08/2011 – Accepted 16/08/2011

Abstract

In this paper, we present an interior penalty formulation for solving equations containing third spatial derivative terms, in the context of a high order spectral volume method. The motivation for this approach comes from the "penalization method" formulated by Kannan and Wang (Kannan R, Wang Z.J., "A Study of Viscous Flux Formulations for a p-Multigrid Spectral Volume Navier Stokes Solver, "Journal of Scientific Computing, 41(2), 2009, 165 - 199) developed for discretizing the second order viscous fluxes. A linear Fourier analysis was performed to compare and contrast the dispersion and the dissipation properties of the new formulation and the existing LDG (Local Discontinuous Galerkin) formulation. The analyses performed on the linear and the cubic partitions showed improvement over the traditional LDG formulation. The analysis performed on the quadratic partition showed significant dispersion, when compared to the LDG scheme. The new formulation is easy to implement and is highly symmetrical. Numerical experiments were conducted and the results were in accord with the analysis results. In general, the formulation is general and can be used even for higher dimension problems.
.

Keywords: Spectral Volume method; LDG; Penalty formulation; Linear Fourier analysis; Stability.

1. Introduction

The spectral volume (SV) method was originally formulated by Wang et al [21,22,23,24,25,16] and further improved by Kannan et al [3,4,5,6,7,9,10,11,12,13,14] for conservation laws on unstructured grids. The spectral volume method is a high order formulation and can be viewed as an extension of the Godunov method to higher order by adding more degrees-of-freedom in the form of subcells in each simplex. Every simplex is comprised of a semi-structured lattice of these subcells. The simplex is referred to as the spectral volume and the subcells are referred to as the control volumes (CV). The degrees of freedom are the CV averaged solutions and are updated using a finite volume procedure.

[c] Corresponding Author: R. Raghavendra
Email: rr0012@uah.edu Tel: +256 417 3339

PII: S2180-1363(11)3274-X

The spectral volume method is akin to the more famous discontinuous Galerkin (DG) [1,2] formulation. The common properties include (i) discontinuous solution space, (ii) possessing multiple degrees of freedom (DOF) within a given element, (iii) capable of providing high order accurate solutions and (iv)compactness. The main difference is on the handling of the DOF: the DG employs the elemental nodal values as DOF, while the spectral volume being a derivative of the finite volume has subcell averages as its DOF.

Yan et al [26,27] implemented the LDG formulation to solve equations containing third order spatial derivative terms in the DG context. Recently, Kannan developed a formulation to solve equations containing third order spatial derivative terms using the LDG (Local Discontinuous Galerkin) formulation [9] in the SV context. The crux of the above formulations was to alternate the direction of the numerical fluxes. Even though both the above works yielded good results, they were not symmetrical. Earlier, Kannan et al [5,12] had proved that the solution can be dependent on the choice of the direction, during his studies involving the LDG scheme for the diffusion equation. It is definitely possible that this phenomenon is possible in the current context.

An interior penalty formulation to discretize the higher order spatial derivative terms is presented in this paper. This approach borrows ideas from the seminal works of Kannan and Wang [5], wherein a length based penalizing factor is used as a penalty term to the central (averaged) flux. Hence this approach is more symmetrical than the LDG approach. Thus the solution is never dependent on the choice of the direction. Kannan and Wang [5] systematically demonstrated that this approach is more accurate than the existing LDG formulation for second derivative terms. A linear Fourier analysis was conducted to compare the diffusion and the dispersion properties of the two formulations. The analyses performed on the linear and the cubic partitions showed improvements over the traditional LDG formulation. The analysis on the quadratic partition showed significant dispersion, when compared to the LDG formulation. Numerical experiments were conducted and their results were in accord with that of the analyses.

The paper is organized as follows. In section 2, we review the basics of the SV method. After that, the LDG and the penalty formulations for high order spatial derivatives are discussed in detail in section 3. A detailed linear analysis is performed for the two formulations in section 4. Numerical results are presented in section 5. The conclusions from this study are summarized in Section 6.

.

2. Basics of the spectral volume method

2.1. The SV method for hyperbolic conservation laws

Consider the general conservation equation

$$\frac{\partial Q}{\partial t}+\frac{\partial (f(Q))}{\partial x}=0, \tag{2.1}$$

where Q is the vector of conserved variables and $f(Q)$ is the vector of fluxes. The Computational domain Ω is discretized into I non overlapping cells called spectral volumes. Each of these spectral volumes are further partitioned into smaller cells called control volumes (CV), denoted by C_{ij}. Figure 1 shows linear, quadratic and cubic partitions in 1D.

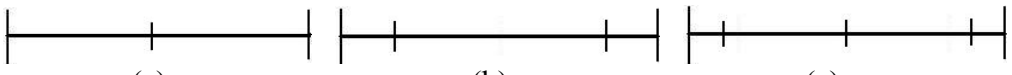

(a) (b) (c)

Figure 1. Partitions of a SV in 1D . Case (a): Linear reconstruction; Case (b): Quadratic reconstruction; Case (c): Cubic reconstruction.

It can be observed that $k+1$ control volume solution averages are required to construct a degree k polynomial. Integration of equation (2.1) over the control volume C_{ij} results in

$$\frac{\partial \overline{Q}_{i,j}}{\partial t} + \frac{1}{V_{i,j}}(F_{i,j+\frac{1}{2}} - F_{i,j-\frac{1}{2}}) = 0, \tag{2.2}$$

where $F_{i,j+\frac{1}{2}}$ is the flux vector through the interface between C_{ij} and C_{ij+1}, $F_{i,j-\frac{1}{2}}$ is the flux vector through the interface between C_{ij} and C_{ij-1} and $\overline{Q}_{i,j}$ is the control volume averaged solution of the control volume C_{ij}. The fluxes in equation (2.2) are obtained from high order reconstructions of the CV averaged conserved variables. In other words, given the CV averaged conserved variables, a degree k polynomial can be constructed such that it is (k+1)th order approximation to Q. In other words, we can write the polynomial as

$$p_i(x) = \sum_{j=1}^{N} L_j(x)\overline{Q}_{i,j}, \tag{2.3}$$

where the shape functions $L_j(x,y)$ satisfy

$$\frac{1}{V_{i,j}} \int_{C_{i,j}} L_n(x)dV = \delta_{j,n}. \tag{2.4}$$

The fluxes are discontinuous across the SV interfaces. Approximate Riemann fluxes like the Rusanov flux [17] or the Roe flux [16] are used to handle the discontinuity.

2.2. The SV method for the diffusion equation

Consider the following diffusion equation, applied inside a domain Ω

$$\frac{\partial u}{\partial t} = \frac{\partial^2 u}{\partial x^2}. \tag{2.5}$$

An auxiliary variable is defined for the gradient:

$$q = \frac{\partial u}{\partial x}. \tag{2.6}$$

The diffusion equation (2.5) becomes

$$\frac{\partial u}{\partial t} = \frac{\partial q}{\partial x}. \tag{2.7}$$

Integrating equations (2.6) and (2.7) and applying the Gauss-divergence theorem,

$$\overline{q}_{ij}V_{ij} = (u_{i,j+\frac{1}{2}} - u_{i,j-\frac{1}{2}}), \tag{2.8}$$

$$\frac{d\overline{u}_{ij}}{dt}V_{ij} = (q_{i,j+\frac{1}{2}} - q_{i,j-\frac{1}{2}}), \tag{2.9}$$

where $\overline{q}_{ij}$ and $\overline{u}_{ij}$ are the CV averaged gradient and solution in C_{ij}. Since the solution is discontinuous at the SV interface, u and q at SV boundaries are replaced by numerical fluxes $\hat{q}$ and $\hat{u}$. Equations (2.8) and (2.9) become

$$\overline{q}_{ij}V_{ij} = (\hat{u}_{i,j+\frac{1}{2}} - \hat{u}_{i,j-\frac{1}{2}}), \tag{2.10}$$

$$\frac{d\overline{u}_{ij}}{dt}V_{ij} = (\hat{q}_{i,j+\frac{1}{2}} - \hat{q}_{i,j-\frac{1}{2}}). \tag{2.11}$$

The LDG approach has been the most common formulation for discretizing the viscous fluxes [20,5]. The numerical fluxes are defined in the following manner:

$$\hat{u} = u_L\,, \tag{2.12}$$

$$\hat{q} = q_R\,, \tag{2.13}$$

where u_L and u_R are the left and right state values of the solution and $\vec{q}_L$ and $\vec{q}_R$ are the left and right state values of the gradients.

The penalty formulation was first implemented by Kannan and Wang [5] in the SV context. This formulation is symmetrical and is given by

$$\hat{u} = \frac{(u_R + u_L)}{2}, \tag{2.14}$$

$$\hat{q} = \frac{(q_R + q_L)}{2} + (u_R - u_L)\vec{n}\frac{A_r}{V_{ij}}, \tag{2.15}$$

where, A_r is the area of the face of the CV in consideration(equals unity in 1D), V_{ij} is the CV volume. More details on this formulation, including its similarity to an approximate Riemann flux, origin and stability can be found in [5].

3. The SV formulation for third order spatial derivatives

Let us consider the following simple linear equation:

$$u_t + u_{xxx} = 0\,. \tag{3.1}$$

The standard procedure is to rewrite equation (3.1) into a first order system [9]:

$$u_t + p_x = 0\,,\ p = q_x\,,\ q = u_x\,. \tag{3.2}$$

Integrating the above equations over the CV results in the below set of equations:

$$\frac{d\overline{u}_{ij}}{dt}V_{ij} + (p_{i,j+\frac{1}{2}} - p_{i,j-\frac{1}{2}}) = 0\,, \tag{3.3}$$

$$\overline{p}_{ij}V_{ij} = (q_{i,j+\frac{1}{2}} - q_{i,j-\frac{1}{2}})\,, \tag{3.4}$$

$$\overline{q}_{ij}V_{ij} = (u_{i,j+\frac{1}{2}} - u_{i,j-\frac{1}{2}})\,. \tag{3.5}$$

u, p and q at SV boundaries are replaced by numerical fluxes $\hat{u}$, $\hat{p}$ and $\hat{q}$.

3.1. The LDG formulation

The LDG formulation for discretizing third order spatial derivatives in a SV context was proposed by Kannan et al [9]. Two choices were reported by Kannan et al [9]:

<u>*Choice a*</u>

$$\hat{u} = u_L\,, \qquad \hat{q} = q_R\,, \hat{p} = \hat{p}_R\,. \tag{3.6}$$

<u>*Choice b*</u>

$$\hat{u} = u_R\,,\ \hat{q} = q_R\,,\ \hat{p} = \hat{p}_L\,. \tag{3.7}$$

3.2. The Interior Penalty formulation

The starting point of the interior penalty formulation is the use of $\hat{u} = u_R$ in equation (3.5), to obtain $\overline{q}$. A high order reconstruction is performed to obtain q on the faces. $\overline{p}$ is computed using two approaches (equation 3.4):

1. The first approach uses a central flux for $\hat{q} = \frac{(q_R + q_L)}{2}$ to obtain $\bar{p}$. This $\bar{p}$ is denoted as $\bar{p}_{AVG}$
2. The second approach uses the q (on the CV faces) from the CV in consideration. This $\bar{p}$ is denoted as $\bar{p}_{SELF}$

A high order reconstruction is performed on $\bar{p}_{AVG}$ to obtain p_{AVG_L} and p_{AVG_R}. p_{SELF_L} and p_{SELF_R} are obtained in a similar manner. Either p_{AVG_L} or p_{AVG_R} can be used for $\hat{p}$ in equation (3.3), for the CV faces which do not lie on the SV boundary (NOTE: $p_{AVG\_L} = p_{AVG\_R}$ for the CV faces, which do not lie on the SV boundary).

The following penalization is used for $\hat{p}$ in equation (3.3), for the CV faces that lie on the SV boundary:

$$\hat{p} = \frac{(p_{SELF\_R} + p_{SELF\_L})}{2} + \frac{\lambda}{2V_i}(q_R - q_L), \tag{3.8}$$

where V_i is the volume of the SV associated with that face and λ is a positive constant. Thus it can be seen that the current formulation displays higher degree of symmetry, though not 100% since the starting step uses $\hat{u} = u_R$ in equation (3.5), to obtain $\bar{q}$.

The starting step can be modified to use $\hat{u} = u_L$. This is equally valid. Averaging (i.e. $\hat{u} = \frac{(u_L + u_R)}{2}$ was found to be unstable.

The motivation behind employing the penalizing term in equation (3.8) arises from Rusanov's approximate Riemann flux. The Rusanov flux comprises of a central flux and a dissipation term. The dissipation term is proportional to the jump between the left and right solution states. It is also proportional to the maximum eigen value of the Jacobian matrix. One can see a connection between the Rusanov flux and equation (3.8). Both have a central component and a dissipation (called penalty in here) component. The Jacobian term however cannot be evaluated analytically for this scenario. So using dimensional analysis, it can be shown that the eigen value has a dimension of 1/length. Hence the form for equation (3.8).

NOTE: Based on the above argument, the only restriction on λ is that it is positive. It cannot predict the magnitude required to make the system stable. This will be determined using a Fourier analysis in the next section in [5].

4. Fourier analysis for the LDG and penalty formulations

In this section, we carry out linear analysis for the LDG and the penalty formulations in 1D. This linear analysis was first employed by Zhang and Shu [28] in the DG setting and later used by Kannan and Wang [5,6,7,9] for studying high order spatial derivatives (second and third). For a given CV averaged solution vector $\lfloor \bar{u}_j \rfloor$ (for the jth SV), linearity and periodicity of the system results in

$$\frac{d}{dt}[\bar{u}_j] = \mathrm{A}[\bar{u}_{j-2}] + \mathrm{B}[\bar{u}_{j-1}] + \mathrm{C}[\bar{u}_j] + \mathrm{D}[\bar{u}_{j+1}] + \mathrm{E}[\bar{u}_{j+2}], \tag{4.1}$$

where A, B, C, D and E are constant matrices. Consider the following Fourier mode

$$u(x,t) = \hat{u}_k(t)e^{ikx}, \tag{4.2}$$

where k is the wave number and $\hat{u}_k$ is the amplitude of the given wave. The analytical solution for equation 3.1 is $u(x,t) = e^{i(kx+k^3t)}$. Using periodicity, the advancement equation can be written as

$$[\hat{u}'_k] = G(k)\,[\hat{u}_k], \tag{4.3}$$

where G is the amplification matrix and is given by

$$G = e^{-2ikh}A + e^{-ikh}B + C + e^{ikh}D + e^{2ikh}E. \tag{4.4}$$

The eigen values of G comprise of the physical (principal eigen value) mode and various spurious modes. The spurious modes are damped much faster than the physical mode (assuming that the scheme is stable).

4.1. Second order spatial analysis

The plot of the real component of the principal eigen value as a function of the non-dimensional frequency ($\xi = kh$) is shown in Figure 2a.

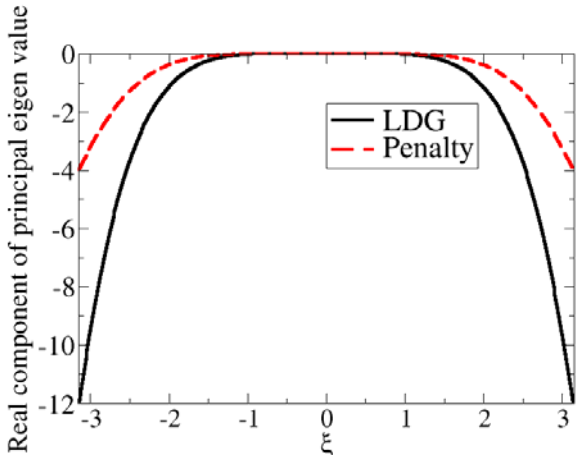

Figure 2a. Real component of the principal eigen value as a function of ξ for the second order SV.

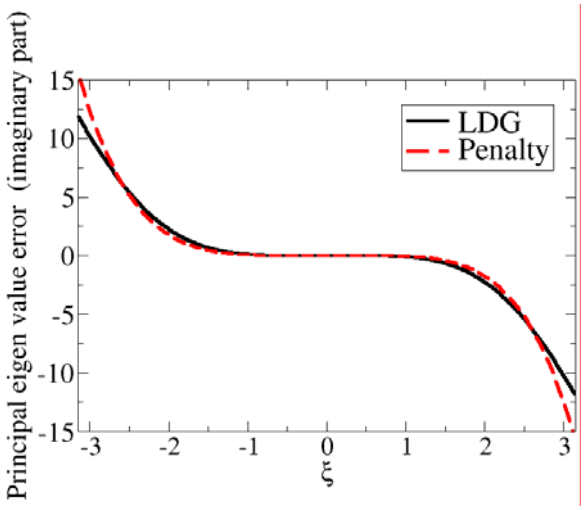

Figure 2b. Error associated with the imaginary component of the principal eigen value as a function of ξ for the second order SV.

All the entries are less than or equal to zero. This implies that the system is stable. It can be seen that the penalty scheme generates smaller numerical dissipation than the LDG scheme. The deviation between the imaginary components of the principal eigen value and the analytical eigen value (i.e. $i\xi^3$) as a function of ξ is plotted in Figure 2b. The penalty scheme is in general comparable the LDG scheme.

A value of 2.0 was used for λ (see equation 3.8). This value was chosen to enable a stable scheme as well as to reduce the dispersion error.

4.2. Third order spatial analysis

Following the notation of Kannan et al [5,9], the third order SV of unit length has its interior CV boundaries given by the following local coordinates: {0, d, 1-d, 1}, where d is the length of the first CV in the SV. A value of d=0.1 was deemed most accurate [5,9]. This will be used in the remainder of the paper.

The plot of the real component of the principal eigen value as a function of the non-dimensional frequency ($\xi = kh$) is shown in Figure 3a. A value of 11.12 was used for λ (see equation 3.8). This value was chosen to enable a stable scheme.

The deviation between the imaginary components of the principal eigen value and the analytical eigen value (i.e. $i\xi^3$) as a function of ξ is plotted in Figure 3b. The dissipation

properties of the LDG and the penalty are comparable. The penalty scheme generates much higher dispersion than the LDG scheme. A higher value of λ mildly alleviates the dispersion errors, but increases the numerical dissipation.

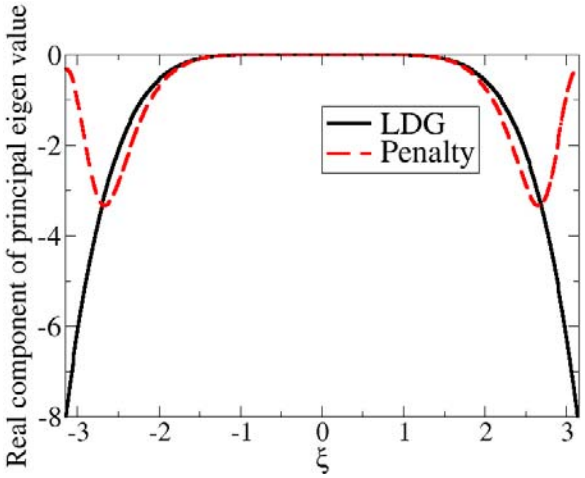

Figure 3a. Real component of the principal eigen value as a function of ξ for the third order SV.

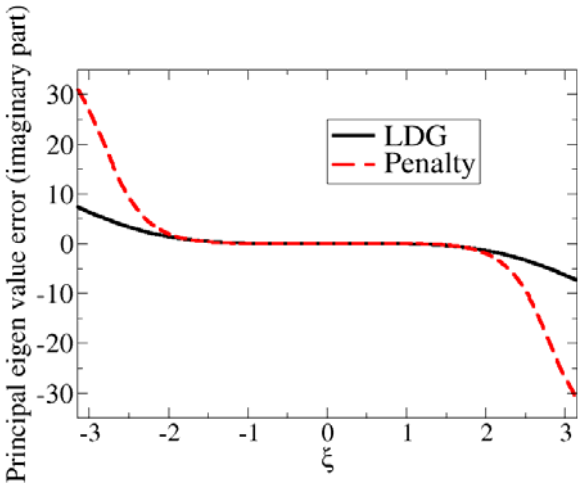

Figure 3b. Error associated with the imaginary component of the principal eigen value as a function of ξ for the third order SV.

4.3. Fourth order spatial analysis

Once again, following the notation of Kannan et al [5,9], the fourth order SV of unit length has its interior CV boundaries given by the following local coordinates: {0, d, 0.5, 1-d, 1}, where d is the length of the first CV in the SV. A value of d=0.1 was deemed most accurate [5,9]. This will be used in the remainder of the paper.

The plot of the real component of the principal eigen value as a function of the ξ is shown in Figure 4a. The system is stable, since all the entries are less than or equal to zero. It can be seen that the penalty scheme generates smaller numerical dissipation than the LDG scheme.

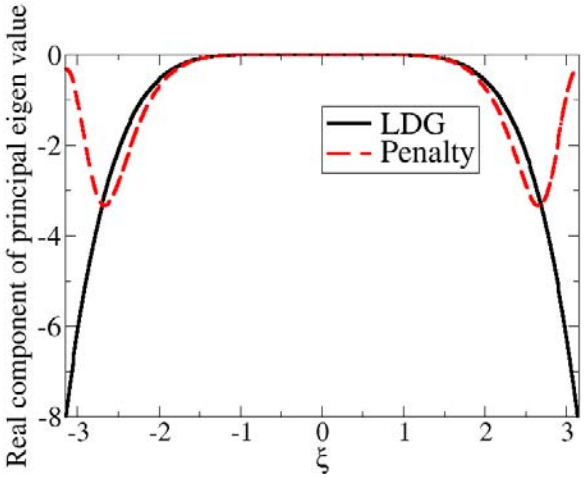

Figure 4a. Real component of the principal eigen value as a function of ξ for the fourth order SV.

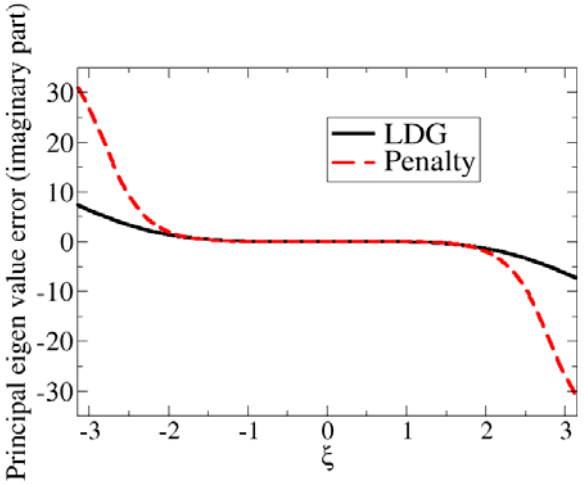

Figure 4b. Error associated with the imaginary component of the principal eigen value as a function of ξ for the fourth order SV.

The deviation between the imaginary components of the principal eigen value and the analytical eigen value (i.e. $i\xi^3$) as a function of ξ is plotted in Figure 4b. The penalty scheme generates smaller dispersion errors than the LDG scheme.

A value of 15.0 was used for λ (see equation 3.8). This value was chosen to enable a stable scheme as well as to reduce the dispersion error.

It must be noted that the Fourier analysis presented assumes plethora of assumptions, including linearity, periodicity and exact time integration. Even though, most of the problems are non-linear and have non-periodic boundary conditions, the Fourier analysis can be considered as a first estimate for ensuring stability (for example by varying λ) and justifying the obtained accuracies (for instance between the LDG and the penalty schemes).

5. Numerical experiments

In this section, the penalty formulation is demonstrated by means of numerical experiments. These are compared with the LDG simulations performed by Kannan et al [9]. A three stage SSP Runge-kutta scheme was used for time advancement [19].

5.1. Test Case 1

An accuracy test is carried out considering the approximate solution of the following equation

$$u_t + u_{xxx} = 0, \tag{5.1}$$

with an initial condition $u(x,0) = \sin(x)$ and periodic boundary conditions over the interval [0, 2π]. This equation has an analytical solution: $u(x,t) = \sin(x+t)$. A non-uniform mesh was used in this study. The mesh had a recurring pattern of SVs of lengths 0.9Δ and 1.1Δ ,where Δ was the length of the corresponding uniform SV. The simulation was performed till $t = 1$ second. The L_2 and L_∞ errors and orders of accuracies were computed at $t = 1$ second and are given in table 1. The corresponding LDG results are also shown. It can be seen that the 2nd and the 4th order penalty simulations yield smaller errors than their LDG counterparts. As expected the error generated by the third order penalty is much higher than its LDG counterpart. In general, the simulations asymptotically attain the desired orders of accuracy.

5.2. Test Case 2

The second test case involved computing the solution of the non-linear KdV equation [9]

$$u_t - 3(u^2)_x + u_{xxx} = 0, \tag{5.2}$$

with an initial condition $u(x,0) = -2sech^2(x)$ over the interval [-10,12]. The boundary conditions are given by

$$u(-10,t) = g_1(t),\ u_x(12,t) = g_2(t),\ u_{xx}(12,t) = g_3(t), \tag{5.3}$$

where $g_i(t)$ is obtained from the analytical solution $u(x,t) = -2sech^2(x-4t)$.

The simulation was performed till $t = 0.5$ second and the non-uniform mesh described the earlier test case was employed. The L_2 and L_∞ errors and orders of accuracies were computed at $t = 0.5$ second and are given in table 2. Once again, it can be seen that the 2nd and the 4th order penalty simulations yield smaller errors than their LDG counterparts and the error generated by the third order penalty is much higher than its LDG counterpart. The simulations asymptotically attain the desired orders of accuracy, in spite of the problem being heavily non-linear.

5.3. Test Case 3

The third test case was designed to test the robustness and accuracy of the method for non-linear problems with small coefficient for the third derivative term [9]

$$u_t + u_x + (\frac{u^4}{4})_x + \varepsilon u_{xxx} = 0, \tag{5.4}$$

with an initial condition $u(x,0) = A sech^{\frac{2}{3}}(K(x - x_0))$, with $A = 0.2275$, $x_0 = 0.5$, $\varepsilon = 2.058e-5$ and $K = 3(\frac{A^3}{40\varepsilon})^{\frac{1}{2}}$. The following boundary conditions were applied over the interval [-2:3]:

$$u(-2,t) = g_1(t),\ u_x(3,t) = g_2(t),\ u_{xx}(3,t) = g_3(t), \tag{5.5}$$

where $g_i(t)$ is obtained from the analytical solution : $u(x,t) = A sech^{\frac{2}{3}}(K(x - x_0) - \omega t)$, where $\omega = K(1 + \frac{A^3}{10})$.

The simulation was performed till $t = 1$ second and the non-uniform mesh described the earlier test case was employed. The L_2 and L_∞ errors and orders of accuracies were computed at $t = 1$ second and are given in table 3. The observations are identical to that of the previous two test cases: the 2nd and the 4th order penalty simulations yield smaller errors than their LDG counterparts and the error generated by the third order penalty is much higher than its LDG counterpart.

5.4. Test Case 4

The fourth test case involves solving a KdV-Burgers equation, on highly non-uniform grids. The equation is given by:

$$u_t + \varepsilon(\frac{u^2}{2})_x - \alpha u_{xx} + \beta u_{xxx} = 0. \tag{5.6}$$

The analytical solution is given by: $u(x,t) = -\frac{3\alpha^2}{25\varepsilon\beta}(-sech^2(kx - ct) + 2\tanh(kc - ct) + 2)$, with $k = \frac{\alpha}{10\beta}$, $c = \frac{3\alpha^3}{125\beta^2}$.

The mesh had a recurring pattern of SVs of lengths 0.5Δ and 1.5Δ ,where Δ was the length of the corresponding uniform SV. The following values were employed for this simulation: $\varepsilon = \alpha = \beta = 1$. This test case has first, second and third derivative spatial fluxes, imbedded non-linearity and is solved on highly non-linear grids. Hence it is a good case to show the robustness and accuracy of the penalty scheme.

The simulation was performed till $t = 1$ second. Upwinding was employed for the first derivative spatial flux. A LDG formulation was employed for the second derivative flux. The L_2 and L_∞ errors and orders of accuracies were computed at $t = 1$ second and are given in table 4. Inspite of the heavy nonlinearity and interaction of the different fluxes, the overall observations are identical to that of the previous two test cases: the 2nd and the 4th order penalty simulations yield smaller errors than their LDG counterparts and the error generated by the third order penalty is much higher than its LDG counterpart.

TABLE 1. $u_t + u_{xxx} = 0 \,.\, u(x,0) = \sin(x)$. L_2 AND L_∞ ORDER AND ERRORS AT T=1.

K	Method	Grid	L_2 error	L_2 order	L_∞ error	L_∞ order
1	LDG	10	1.60e-2	-	5.83e-2	-
		20	4.08e-3	1.97	1.56e-2	1.90
		40	1.03e-3	1.99	3.96e-3	1.98
		80	2.57e-4	2.00	9.97e-4	1.99
1	Penalty	10	8.32e-3	-	3.15e-2	-
		20	2.09e-3	1.99	8.15e-3	1.95
		40	5.24e-4	2.00	2.05e-3	1.99
		80	1.31e-4	2.00	5.13e-4	2.00
2	LDG	10	8.81e-4	-	4.47e-3	-
		20	1.12e-4	2.97	5.74e-4	2.96
		40	1.41e-5	2.99	7.28e-5	2.98
		80	1.77e-6	3.00	9.16e-6	2.99
2	Penalty	10	2.73e-3	-	1.47e-2	-
		20	5.90e-4	2.21	3.65e-3	2.01
		40	1.06e-4	2.47	8.00e-4	2.19
		80	1.55e-5	2.78	1.53e-4	2.39
3	LDG	10	5.11e-5	-	2.41e-4	-
		20	3.26e-6	3.97	1.55e-5	3.96
		40	2.06e-7	3.98	9.81e-7	3.98
		80	1.30e-8	3.99	6.22e-8	3.98
3	Penalty	10	3.11e-5	-	1.57e-4	-
		20	1.96e-6	3.99	9.88e-6	3.99
		40	1.22e-7	4.00	6.17e-7	4.00
		80	7.65e-9	4.00	3.86e-8	4.00

TABLE 2. $u_t - 3(u^2)_x + u_{xxx} = 0 \,.\, u(x,0) = -2sech^2(x)$. L_2 AND L_∞ ERRORS AT T=0.5.

k	Method	Grid	L_2 error	L_2 order	L_∞ error	L_∞ order
1	LDG	10	2.62e-1	-	1.46e-0	-
		20	8.53e-2	1.62	6.01e-1	1.28
		40	2.50e-2	1.77	2.20e-1	1.45
		80	6.71e-3	1.90	7.11e-2	1.63
		160	1.72e-3	1.96	2.08e-2	1.77
		320	4.31e-4	2.00	5.47e-3	1.93
1	Penalty	10	1.44e-1	-	8.61e-1	-
		20	4.49e-2	1.68	3.28e-1	1.39
		40	1.26e-2	1.83	1.09e-1	1.59
		80	3.27e-3	1.95	3.33e-2	1.71
		160	8.24e-4	1.99	9.44e-3	1.82
		320	2.06e-4	2.00	2.39e-3	1.98
2	LDG	10	1.09e-1	-	1.06e0	-
		20	1.66e-2	2.71	1.65e-1	2.68
		40	2.51e-3	2.73	2.81e-2	2.56

		80	3.43e-4	2.87	4.57e-3	2.62
		160	4.41e-5	2.96	6.51e-4	2.81
		320	5.51e-6	3.00	8.31e-5	2.97
2	Penalty	10	3.59e-1	-	3.89e-0	-
		20	6.94e-2	2.37	8.41e-1	2.21
		40	1.15e-2	2.59	1.63e-1	2.37
		80	1.70e-3	2.76	2.86e-2	2.51
		160	2.41e-4	2.82	4.30e-3	2.73
		320	3.16e-5	2.93	5.73e-4	2.91
3	LDG	10	4.99e-2	-	4.09e-1	-
		20	5.18e-3	3.27	4.83e-2	3.08
		40	4.77e-4	3.44	4.81e-3	3.33
		80	3.45e-5	3.79	4.34e-4	3.47
		160	2.25e-6	3.94	3.20e-5	3.76
		320	1.42e-7	3.98	2.04e-6	3.97
3	Penalty	10	3.29e-2	-	2.53e-1	-
		20	3.12e-3	3.40	2.79e-2	3.18
		40	2.70e-4	3.53	2.63e-3	3.41
		80	1.91e-5	3.82	2.12e-4	3.63
		160	1.25e-6	3.93	1.44e-5	3.88
		320	7.89e-8	3.99	9.13e-7	3.98

TABLE 3. $u_t + u_x + (\frac{u^4}{4})_x + \varepsilon u_{xxx} = 0 \,.\, u(x,0) = A sech^{\frac{2}{3}}(K(x - x_0))$. L_2 AND L_∞ ERRORS AT T=1.

k	**Method**	**Grid**	**L_2 error**	**L_2 order**	**L_∞ error**	**L_∞ order**
1	LDG	10	4.45e-2	-	4.15e-1	-
		20	1.74e-2	1.35	1.74e-1	1.25
		40	6.17e-3	1.50	6.99e-2	1.32
		80	1.90e-3	1.70	2.56e-2	1.45
		160	5.38e-4	1.82	8.56e-3	1.58
		320	1.38e-4	1.96	2.44e-3	1.81
		640	3.46e-5	2.00	6.23e-4	1.97
1	Penalty	10	2.00e-2	-	2.03e-1	-
		20	7.37e-3	1.44	8.18e-2	1.31
		40	2.38e-3	1.63	3.06e-2	1.42
		80	6.61e-4	1.85	1.01e-2	1.60
		160	1.70e-4	1.96	2.96e-3	1.77
		320	4.27e-5	1.99	7.87e-4	1.91
		640	1.07e-5	2.00	2.00e-4	1.98
2	LDG	10	2.53e-2	-	2.09e-1	-
		20	4.61e-3	2.46	4.32e-2	2.28
		40	9.17e-4	2.33	9.27e-3	2.22
		80	1.77e-4	2.37	1.84e-3	2.33
		160	2.69e-5	2.72	3.32e-4	2.47
		320	3.51e-6	2.94	4.77e-5	2.80
		640	4.45e-7	2.98	6.10e-6	2.97
2	Penalty	10	6.83e-2	-	4.59e-1	-
		20	1.40e-2	2.29	1.05e-1	2.13
		40	2.73e-3	2.35	2.23e-2	2.23
		80	4.91e-4	2.48	4.38e-3	2.35

		160	7.45e-5	2.72	7.38e-4	2.57
		320	9.91e-6	2.91	1.07e-4	2.78
		640	1.26e-6	2.97	1.39e-5	2.95
3	LDG	10	2.09e-2	-	1.85e-1	-
		20	2.57e-3	3.03	2.85e-2	2.70
		40	2.37e-4	3.44	3.64e-3	2.97
		80	1.76e-5	3.75	3.70e-4	3.30
		160	1.18e-6	3.90	2.83e-5	3.71
		320	7.47e-8	3.98	1.92e-6	3.88
		640	4.67e-9	4.00	1.21e-7	3.99
3	Penalty	10	1.15e-2	-	9.44e-2	-
		20	1.23e-3	3.23	1.22e-2	2.95
		40	1.02e-4	3.59	1.36e-3	3.17
		80	7.31e-6	3.80	1.12e-4	3.59
		160	4.73e-7	3.95	8.09e-6	3.80
		320	2.99e-8	3.99	5.20e-7	3.96
		640	1.86e-9	4.00	3.27e-8	3.99

TABLE 4. $u_t + \varepsilon(\frac{u^2}{2})_x - \alpha u_{xx} + \beta u_{xxx} = 0$. $u(x,0) = -\frac{3\alpha^2}{25\varepsilon\beta}(-sech^2(kx) + 2\tanh(kc) + 2)$. L_2 AND L_∞ ERRORS AT T=1.

k	**Method**	**Grid**	**L_2 error**	**L_2 order**	**L_∞ error**	**L_∞ order**
1	LDG	40	2.11e-3	-	3.26e-2	-
		80	7.21e-4	1.55	1.28e-2	1.35
		160	2.10e-4	1.78	3.99e-3	1.68
		320	5.47e-5	1.94	1.06e-3	1.91
1	Penalty	40	1.28e-3	-	1.76e-2	-
		80	4.02e-4	1.67	6.18e-3	1.51
		160	1.07e-4	1.91	1.75e-3	1.82
		320	2.65e-5	1.99	4.56e-4	1.94
2	LDG	40	3.22e-4	-	5.44e-3	-
		80	5.50e-5	2.55	1.09e-3	2.32
		160	8.40e-6	2.71	1.74e-4	2.65
		320	1.10e-6	2.93	2.36e-5	2.88
2	Penalty	40	6.11e-4	-	1.11e-2	-
		80	1.23e-4	2.31	2.57e-3	2.11
		160	2.13e-5	2.53	4.97e-4	2.37
		320	3.13e-6	2.77	7.71e-5	2.69
3	LDG	40	5.11e-5	-	7.89e-4	-
		80	5.45e-6	3.23	9.67e-5	3.03
		160	4.37e-7	3.64	8.72e-6	3.47
		320	2.79e-8	3.97	5.80e-7	3.91
3	Penalty	40	4.05e-5	-	5.11e-4	-
		80	4.14e-6	3.29	5.80e-5	3.14
		160	2.99e-7	3.79	4.60e-6	3.66
		320	1.88e-8	3.99	2.92e-7	3.97

6. Conclusion

An interior penalty formulation was implemented for solving equations containing third spatial derivative terms in a spectral volume context. This is different from the existing LDG formulation, wherein the fluxes are obtained by alternating the left and right state values. This makes the penalty formulation definitely symmetrical (This is similar to Kannan and Wang's symmetrical penalty formulation for second derivative terms [5]). The magnitude of the required penalizing term was determined using a linear Fourier analysis, at the stability limit. The dispersion and the dissipation properties of this new formulation and the existing LDG formulation were studied using the linear Fourier analysis. The analysis showed that the new formulation is more accurate than the LDG formulation for the second and fourth order simulations (i.e. linear and cubic partitions). The high dispersion error present in the third order (quadratic partition) interior penalty formulation, results in the LDG being a better choice for third order simulations.

Numerical experiments were performed to assess the new formulation. The observations from these experiments were in accord with those of the analyses: the 2^{nd} and the 4^{th} order penalty simulations yield smaller errors than their LDG counterparts and the error generated by the third order penalty is much higher than its LDG counterpart. Both the linear and the non-linear equations attained the expected orders of accuracy asymptotically.

Kannan and Wang were able to improve their LDG results using LDG2 [13], an intelligently formulated variant of the LDG method. The LDG2 uses a combination of one sided derivatives and central derivatives. This idea can also be used in the penalty formulation: using a combination of the existing penalty and a central flux. Rigorous testing of the above is underway and will be reported in future publications.

Other future work will include extension to fourth and fifth order spatial derivative terms, extension to 2D problems and implementing the extremely efficient implicit time discretization procedures developed by Liang et al [15].

References

[1] B. Cockburn and C. W. Shu. *Runge-Kutta discontinuous Galerkin methods for convection-dominated problems*. Journal of Scientific Computing, Sep 2001. **16**(3): p. 173–261.

[2] B. Cockburn and C.W. Shu. *The local discontinuous Galerkin method for time-dependent convection diffusion system*. SIAM Journal of Numerical. Analysis, 1998. 35 p. 2440–2463.

[3] R. Kannan. *An Implicit LU-SGS Spectral Volume Method for the Moment Models in Device Simulations: Formulation in 1D and application to a p-multigrid algorithm.* International Journal for Numerical Methods in Biomedical Engineering (formerly Communications in numerical methods in engineering), Published Online: 1 Feb 2010 (DOI: 10.1002/cnm.1359)

[4] R. Kannan. *An Implicit LU-SGS Spectral Volume Method for the Moment Models in Device Simulations II: Accuracy studies and performance enhancements using the penalty and the BR2 formulations*. International Journal for Numerical Methods in Biomedical Engineering (formerly Communications in numerical methods in engineering), (DOI: 10.1002/cnm.1415)

[5] R. Kannan and Z.J. Wang. *A study of viscous flux formulations for a p-multigrid spectral volume Navier stokes solver*. Journal of Scientific Computing, 2009. **41**(2): p.165-199.

[6] R. Kannan and Z.J. Wang. *LDG2: A variant of the LDG viscous flux formulation for the Spectral Volume method*. Journal of Scientific Computing, 2011. **46**(2) p. 314-328.

[7] R. Kannan and Z.J. Wang. *The Direct Discontinuous Galerkin (DDG) viscous flux scheme for the High Order Spectral Volume method*. Computers and Fluids, 2010. **39**(10) p. 2007-2021.

[8] R. Kannan and Z.J. Wang. *Curvature and Entropy Based Wall Boundary Condition for the High Order Spectral Volume Euler Solver*. Computers and Fluids 2011. **44**(1) p. 79-88.

[9] R. Kannan R. *A High Order Spectral Volume formulation for solving equations containing higher spatial derivative terms: Formulation and analysis for third derivative spatial terms using the LDG discretization procedure*. Communications in Computational Physics, 2011. 10(5) p. 1257-1279.

[10] R. Kannan and Z.J. Wang. *A high order Spectral Volume method for moving boundary problems*. 40th Fluid Dynamics Conference and Exhibit 2010. AIAA 2010-4992.

[11] R. Kannan. *A High Order Spectral Volume Method for Elastohydrodynamic Lubrication problems: formulation and application of an implicit p-multigrid algorithm for line contact problems*. Computers and Fluids, 2011. **48**(1) p. 44-53.

[12] R. Kannan, *High order spectral volume and spectral difference methods on unstructured grids*. Thesis (Ph.D.)--Iowa State University, 2008. Publication Number: AAI3342262; ISBN: 9780549997177; Source: Dissertation Abstracts International, Volume: 70-01, Section: B, page: 0437.; 137 p.

[13] R. Kannan. *A High Order Spectral Volume formulation for solving equations containing higher spatial derivative terms II: Improving the third derivative spatial discretization using the LDG2 method*. Communications in Computational Physics, (submitted).

[14] R. Kannan and Z.J. Wang. *A high order spectral volume solution to the Burgers' equation using the Hopf–Cole transformation*. International Journal for Numerical Methods in Fluids, DOI: 10.1002/fld.2612

[15] C. Liang, R. Kannan and Z.J. Wang. *A-p-multigrid Spectral Difference method with explicit and implicit smoothers on unstructured grids*. Computers & Fluids, 2009. **38**(2) p. 254-265.

[16] Y. Liu, M. Vinokur and Z.J. Wang. *Spectral (finite) volume method for conservation laws on unstructured grids V: extension to three-dimensional systems*. Journal of Computational Physics, 2006. **212**(2) p.454–472.

[17] P.L. Roe. *Approximate Riemann solvers, parameter vectors and difference schemes.* Journal of Computational Physics 1981. **43**(2) p. 357–372.

[18] V.V. Rusanov. *Calculation of interaction of non-steady shock waves with obstacles*. J. Comput. Math. Phys, 1961**.** USSR **1** (1961) p. 267-279.

[19] C.W. Shu. *Total-variation-diminishing time discretizations*. SIAM Journal on Scientific and Statistical Computing, 1988. **9**(6) p. 1073–1084.

[20] Y. Sun, Z.J. Wang and Y. Liu. *Spectral (finite) volume method for conservation laws on unstructured grids VI: Extension to viscous flow*. Journal of Computational Physics, 2006. **215**(1) p.41-58.

[21] Z.J. Wang. *Spectral (finite) volume method for conservation laws on unstructured grids: basic formulation*. Journal of Computational Physics, 2002. **178**(1) p. 210-251.

[22] Z.J. Wang and Y. Liu. *Spectral (finite) volume method for conservation laws on unstructured grids II: extension to two-dimensional scalar equation*. Journal of Computational Physics, 2002. **179** (2) p. 665-697.

[23] Z.J. Wang and Y. Liu. *Spectral (finite) volume method for conservation laws on unstructured grids III: extension to one-dimensional systems*. Journal of Scientific Computing, 2004. **20**(1) p. 137-157.

[24] Z.J. Wang and Y. Liu. *Spectral (finite) volume method for conservation laws on unstructured grids IV: extension to two-dimensional Euler equations*. Journal of Computational Physics, 2004. **194** (2) p. 716-741.

[25] Z.J. Wang and Y. Liu. *Extension of the spectral volume method to high-order boundary representation*. Journal of Computational Physics, 2006. **211**(1) p. 154–178.

[26] J. Yan and C.W. Shu. *A local discontinuous Galerkin method for KdV type equations*. SIAM J. NUMER. ANAL, 2003. **40**(2) p. 769–791.

[27] J. Yan and H. Liu. *A local discontinuous Galerkin method for the Korteweg–de Vries equation with boundary effect*. Journal of Computational Physics, 2006. **215**(1) p. 197-218.

[28] M. Zhang and C.W. Shu. *An analysis of three different formulations of the discontinuous Galerkin method for diffusion equations*. Mathematical Models and Methods in Applied Sciences, 2003. **13**(3) p. 395-413.